Terra Nova

doi: 10.1111/ter.12225

# Metamorphic sole formation, emplacement and blueschist facies overprint: early subduction dynamics witnessed by western Turkey ophiolites

Alexis Plunder,[1,2] Philippe Agard,[1,2,3] Christian Chopin,[4] Mathieu Soret,[1,2] Aral I. Okay[5] and Hubert Whitechurch[6]

[1]*Sorbonne Universités, UPMC Univ Paris 06, CNRS, Institut des Sciences de la Terre de Paris (ISTeP), 4 place Jussieu, Paris 75005, France;* [2]*CNRS, UMR 7193, ISTeP, Paris F-75005, France;* [3]*IUF, Paris F-75005, France;* [4]*Laboratoire de Géologie, Ecole Normale Supérieure – CNRS, UMR 8538, 24 rue Lhomond, Paris 75005, France;* [5]*Eurasia Institute of Earth Sciences and Department of Geology, Istanbul Technical University, Maslak, Istanbul 34469, Turkey;* [6]*Université de Strasbourg, 1 rue Blessig, Strasbourg Cedex 67084, France*

## ABSTRACT

**The largest ophiolite on Earth, in western Turkey, is a key place to study obduction and early subduction dynamics. Ophiolite remnants derived from the same Neotethyan branch (preserved as a result of long-lived Late Cretaceous continental subduction and later obduction) are underlain by hundred-metre-thick extensive metamorphic soles. These soles formed synchronously, at *c*. 93 Ma, and were welded to the base of the ophiolite, thereby dating the start of intra-oceanic subduction. This contribution focuses on the structure, petrology and pressure–temperature evolution of the soles and other subduction-derived units. Peak pressure–temperature conditions were estimated at 10.5 ± 2 kbar and 800 ± 50 °C for the sole by means of pseudosection calculations using Theriak/Domino and at 12 kbar and 425 °C for the unique, enigmatic blueschist facies overprint of the sole. This study provides clues to the mechanisms of sole underplating during early subduction, later cooling, and the nature of the western Turkey ophiolite.**

Terra Nova, 28: 329–339, 2016

## Introduction

Western Turkey offers an exceptionally large (>200 km), unmetamorphosed and well-preserved ophiolite, enabling subduction dynamics and obduction to be studied. Following the classic paper of Şengör and Yılmaz (1981), western Turkey ophiolites are believed to derive from the same Neotethyan realm (with diverse palaeogeographic reconstructions: Şengör and Yılmaz, 1981; Barrier and Vrielynck, 2008; van Hinsbergen *et al*., 2010, 2016; Pourteau *et al*., 2016). No suture zone has been found in between the continental fragments successively accreted over 40 Ma (Tavşanlı, Afyon, Menderes; van Hinsbergen *et al*., 2010).

Models advocating a single ophiolite nappe are supported by the existence of metamorphic soles (hereafter MS) with similar cooling ages (*c*. 93 Ma) under most Anatolian ophiolite fragments (Dilek *et al*., 1999; Önen, 2003; Çelik *et al*., 2006). This places strong constraints on intra-oceanic subduction initiation, because MS derive from the downgoing plate, are metamorphosed at depths of 25 ± 10 km and become welded to the upper-plate ophiolite during a short time span (*c*. 0–2 Ma; Hacker, 1994; Whitechurch *et al*., 1984), in the warm geotherm accompanying intra-oceanic subduction initiation.

Fundamental mechanisms of MS formation, however, remain ill-constrained: knowledge of pressure–temperature (*PT*) conditions and regional-scale variations is poor (Spray, 1984; Wakabayashi and Dilek, 2003; Dewey and Casey, 2013; van Hinsbergen *et al*., 2015, Agard *et al*., 2016) and emplacement mechanisms below the ophiolite are unknown (i.e. how soles are welded to the ophiolite and/or how to reconcile the mismatch between the *PT* conditions of the MS and the ophiolite thickness (Hacker and Gnos, 1997).

This study investigates the following regional and fundamental issues:

1 Did all MS form under similar *PT* conditions? (Published estimates worldwide are sparse and rely on contrasting methods; Agard et al., 2016.)
2 The Turkish ophiolite exemplifies one of the unresolved issues about MS formation: how can MS be welded below the undeformed ophiolite across more than 200 km if they originate from the same depths (or even a depth range between 15 and 30 km) and formed within *c*. 1 Ma of subduction initiation? (Note that this depth time frame is compatible with common values for convergence velocities, i.e. 1–5 cm $a^{-1}$).
3 Turkish MS contain an enigmatic and almost unique blueschist facies overprint in places (Dilek and Whitney, 1997; Okay *et al*., 1998), elsewhere reported only from the northern Cascades (Brown *et al*., 1982), whose *PT* conditions and distribution are still poorly documented. Does the blueschist facies overprint result from a re-subduction of the MS (Dilek and Whitney, 1997) or from later cooling (Okay *et al*., 1998)? What is the link between the MS overprint (and its extent) and the underlying subducted oceanic units, and what are the implications for early subduction dynamics?

This field-based study aims to answer these questions by characterizing the *PT* conditions of the MS and underlying units, assessing their mutual

Correspondence: Alexis Plunder, Department of Earth Sciences, Utrecht University, Heidelberglaan 2, Utrecht 3584CS, The Netherlands. E-mail: a.v.plunder@uu.nl

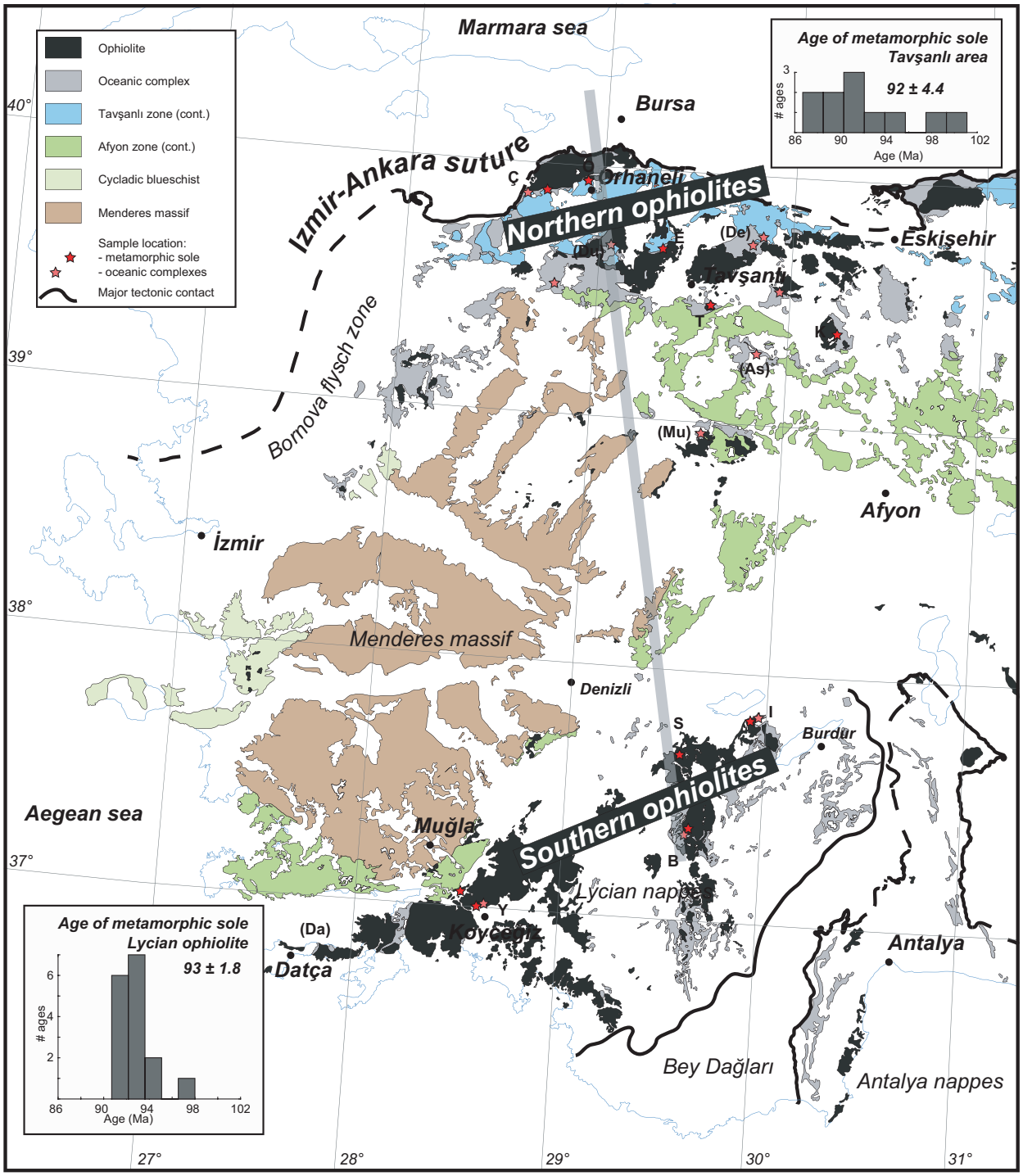


**Fig. 1** Simplified geological map of western Turkey showing the units of the studied area with sample localities. Abbreviation in brackets corresponds to locations where no metamorphic sole was found. Cooling ages of the metamorphic sole are reported for the northern and southern areas after Thuizat *et al.*, 1981; Harris *et al.*, 1994; Önen, 2003; Çelik *et al.*, 2006; and Çelik, 2008. O, Orhaneli; Ç, Çivili; Du: Dutluca; E, Elmaağacı; De, Devlez; T, Tavşanlı; K, Kütahya; As, Aslapana; Mu, Murat Dağı; I, Iğdır; S, Salda; B, Belkaya; Y, Yayla; Da, Datça. Map is modified from the maps of the MTA (Geological Survey of Turkey, 2002 editions).

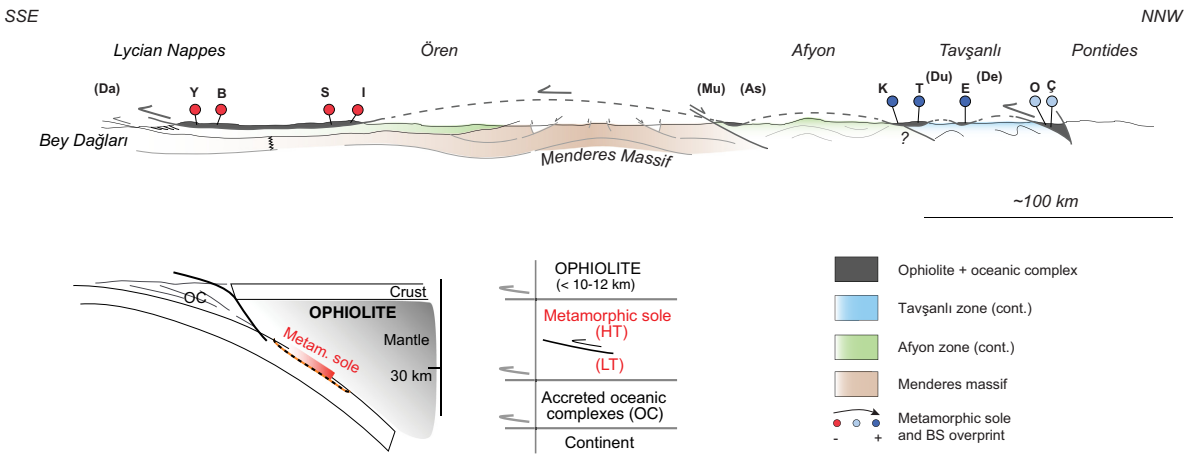


**Fig. 2** Schematic cross-section of western Turkey. MS samples location are indicated. The colour indicates the extent of BS overprint. Location is indicated in Fig. 1. Schematic section at *c*. 95 Ma or shortly after, and simplified section showing the overall organization of the discussed units.

**Table 1** Compilation of information about the ophiolite, the metamorphic sole and the underlying accreted oceanic units. References: 1, Collins and Robertson (1997); 2, Manav *et al.* (2004); 3, Okay *et al.* (1998); 4, Çelik and Chiaradia (2008); 5, Önen (2003); 6, Çelik *et al.* (2006); 7, Önen and Hall (1993); 8, Harris *et al.* (1994); 9, Önen and Hall (2000); 10, Plunder *et al.* (2015).

| | Yayla | Belkaya | Salda | Iğdır | Tavşanlı | Kütahya | Elmaağaacı | Orhaneli | Çivili |
|---|---|---|---|---|---|---|---|---|---|
| Ophiolite | | | | | | | | | |
| Thickness | ~2 km[1] | ~2 km[1] | ~2 km[1] | ~2 km[1] | ~0.5 km | Unknown | ~2 km[2] | ~13 km[3] | ~13 km[3] |
| Presence of crust | No | No | No | No | No | No | No | No | No |
| Dyke | Yes | Yes | Dated: 63–81 Ma[4] | Yes | Yes | Dated: 79 Ma[5] | Yes | Yes | Yes |
| Metamorphic sole | | | | | | | | | |
| Thickness | ~200 m | ~100 m | ~100–200 m | ~100–200 m | ~500 m | ~150–200 m | ~20 m | ~150–200 m[3] | ~150–200 m[3] |
| Age | 93 ± 0.9 Ma[6] | Unknown | 91 ± 0.9 Ma[6] | Unknown | Unknown | 93 ± 2 Ma[7] | Unknown | 101 ± 3.8 Ma[8] | Unknown |
| HT/LT | HT & LT | HT | HT & LT | HT | HT | HT & LT | HT | HT | HT |
| Mineralogy | grt–amph | grt–amph | grt–amph or cpx–amph | grt–amph–cpx | grt–amph | grt–amph–cpx | grt–amph | grt–amph | grt–amph–cpx |
| *PT* | 650 °C[4] | Unknown | 3 kbar and 650 °C[4] | Unknown | Unknown | 3.5 ± 1.5 kbar 700 ± 100 °C[9] | Unknown | 8.5 ± 3 kbar and 700 ± 50 °C[3] | 8.5 ± 3 kbar and 700 ± 50 °C[3] 11 ± 1.5 kbar and 725 ± 50 °C[10] |
| BS overprint | No | No | No | No | Y (strong) | Y (small) | Y (strong) | Y (small) | Y (small) |
| BS mineralogy | | | | | gln–lws–NaPx | gln | gln–lws–jd | lws | gln–lws |
| Basement | | | | | | | | | |
| OC1 or OC1* | OC1 | OC1 | OC1 | OC1 | OC1* | OC1* | | OC1/OC1* | OC1/OC1* |
| OC2 | | | | | OC2 | OC2 | OC2 | | |
| Continent | Lycian nappes | Lycian nappes | Lycian nappes | Lycian nappes | Tavşanlı / Ayon? | Tavşanlı / Ayon? | Tavşanlı | Tavşanlı | Tavşanlı |

relationships, understanding the (early) subduction dynamics and discussing the nature of the ophiolite nappe.

## Geological setting

The western Turkey ophiolite roots in the Izmir-Ankara suture zone, the remnant of a major Neotethyan branch separating Eurasia and the Gondwana-derived Anatolide-Tauride Block (Okay and Tüysüz, 1999). Ophiolite fragments were emplaced atop the Anatolide-Tauride Block following northward-dipping intra-oceanic subduction and later continental subduction below an oceanic plate ('obduction' *sensu stricto*). The resulting nappe stack comprises, from top to bottom: the ophiolite with its MS beneath, accreted oceanic units (or accretionary prism, often referred to as mélange) and continent-derived units (Figs 1 and 2). Age constraints indicate that all MS formed synchronously a few Ma prior to 93 Ma (Çelik *et al.*, 2011;

 

only two discordant ages exist: 82 Ma and 104 Ma; Daşçı *et al.*, 2014 and Harris *et al.*, 1994 respectively). Ophiolite bodies so far described are dominantly harzburgite and dunite (Lisenbee, 1972; Manav *et al.*, 2004), hosting late *c.* 63–89 Ma isolated diabase dykes (Parlak and Delaloye, 1996; Önen, 2003; Çelik and Chiaradia, 2008). Lower Eocene (in the north: Baş, 1986; Özgen-Erdem *et al.*, 2007) and Palaeocene limestones (in the south: Poisson, 1977) unconformably overlie the ophiolite. An assessment of a common origin of all ophiolite klippen is hampered, however, by the almost complete lack of crustal sequence. The geographic distribution only allows for the distinction of a northern and a southern ophiolite group (Fig. 1).

The Anatolide-Tauride Block represents a continuous nappe stack. It is divided into several units, with, from top to bottom and north to south:

1 the blueschist to eclogite facies Tavşanlı zone metamorphosed at *c.* 80–90 Ma (Okay *et al.*, 1998);
2 the low-grade blueschist facies Afyon-Ören-Bolkardag zone metamorphosed at around 65 Ma (Candan *et al.*, 2005; Pourteau *et al.*, 2013, 2014);
3 the Menderes Massif, representing a stack of Alpine and partly Pan-African units (Dora *et al.*, 2001; Gessner *et al.*, 2004) metamorphosed at *c.* 34–44 Ma; and
4 the Lycian nappes, a non-metamorphic equivalent of the Ören zone, emplaced atop the Tauride platform, which correspond to a stack of non-metamorphic to low-grade thrust sheets emplaced from the Maastrichtian to the Miocene (de Graciansky, 1972; Collins and Robertson, 1998; Pourteau *et al.*, 2010).

## Sub-ophiolitic units: metamorphic soles and accreted oceanic units

Here, we provide field relationships between the peridotite, the MS and the oceanic units accreted underneath them (Table 1; Appendix S1 and Table S1). Below, we present the results of a systematic sampling across this transect.

Oceanic rocks from the accretionary prism can be divided into three gradational major units: virtually non-metamorphic (OC1), blueschist facies (OC2) and high-grade blueschist facies (OC3). OC3 is only found locally in the NE with *PT* conditions of ~17 kbar and 450 °C (Plunder *et al.*, 2015) and is not described here. Microscopic observations reveal subtle metamorphic differences in OC1 that may allow further metamorphic grade subdivisions. However, these remain hard to establish in the field (Okay, 1982; Topuz *et al.*, 2006). Petrological characteristics of the MS, OC1 and OC2 units observed below the ophiolite of the Tavşanlı and Lycian regions are described below. Analytical procedures and mineral analysis can be found in Appendix S1 and Table S2.

### Metamorphic sole

The high-temperature (H*T*) part of the MS is mainly made of metabasalt. The general dip of the foliation is parallel to the contact with the peridotite. Hand samples show strong flattening deformation with tight folding. The overall thickness of the MS is ~100–200 m, with half consisting of H*T* amphibolite (Table 1). The greenschist facies section, wherever present, consists of intercalated mafic and sedimentary rocks. Northern MS show variable degrees of blueschist overprint: metabasite turns bluish (Fig. 3a) and the overprint is conspicuous in former plagiogranite with the development of blue amphibole and sodic pyroxene in late veins. No pervasive deformation was associated with the overprint.

Petrographic observation reveals that the amphibolite facies paragenesis consists of amphibole, plagioclase and garnet ± clinopyroxene ± quartz as major phases. Rutile reacting to titanite was found included in garnet and amphibole. Ilmenite was observed reacting to titanite. Garnet and garnet–clinopyroxene-bearing amphibolite and blueschist overprinted samples were preferentially investigated. In some samples, clinopyroxene and garnet form intergrowths (Fig. 3c,d). Amphibole and plagioclase were found included in clinopyroxene and garnet, showing that they are part of the peak paragenesis. Clinopyroxene has a composition of diopside with an Mg# (=Mg/(Mg+Fe)) of 0.65 (KU1308a) or 0.80 (YE1302b). The Na content of clinopyroxene is ~0.10–0.14 per formula unit (p.f.u.). Garnet has a composition between the grossular and almandine end-members with constant pyrope and spessartine contents (Fig. 4b). The pyrope content is higher in clinopyroxene-bearing samples ($0.16 < X_{Pyrope} < 0.28$). The amphibole composition varies between pargasite and hornblende and the Ti content ranges from 0.05 to 0.25 p.f.u. with no relation to the texture (matrix vs. inclusion). Amphibole displays greenschist (actinolite) or blueschist facies (glaucophane) static overgrowths depending on the locality. When preserved, plagioclase composition is $An_{20-30}$. Plagioclase is generally altered into turbid albite + lawsonite (north) or albite + epidote ± muscovite (south) aggregates depending on the blueschist overprint. Jadeite was found coexisting with quartz and lawsonite in former

**Fig. 3** Hand sample, petrographic and backscattered-electron views of samples from the metamorphic sole, the OC1 and the OC1* units. (a) Strongly overprinted metamorphic sole. (b) Thin-section view of an overprinted metamorphic sole. Garnet is almost entirely retrogressed and replaced by a mixture of brownish chlorite and tiny rectangular lawsonite crystals. Blue amphibole overgrows the green ones. (c,d) High-temperature metamorphic sole showing garnet–clinopyroxene globular texture. Plagioclase is indicated by white arrows. (e) Photograph of a hydrothermally altered basalt sample. The feldspar shape can still be identified, but it is now made of albite. (f) Backscattered-electron image of a slightly metamorphosed basalt (OC1*). Lawsonite needles grow in former plagioclase. Magmatic pyroxene shows light-coloured rims consisting of sodic pyroxene. Epidote shows the first stage of hydrothermal alteration. (g) Photograph and (h) backscattered-electron image of the preserved magmatic texture and development of high-pressure minerals in a basalt sample of OC1*. Mineral abbreviations after Kretz (1983) except for Amph, Amphibole and Phg, Phengite.

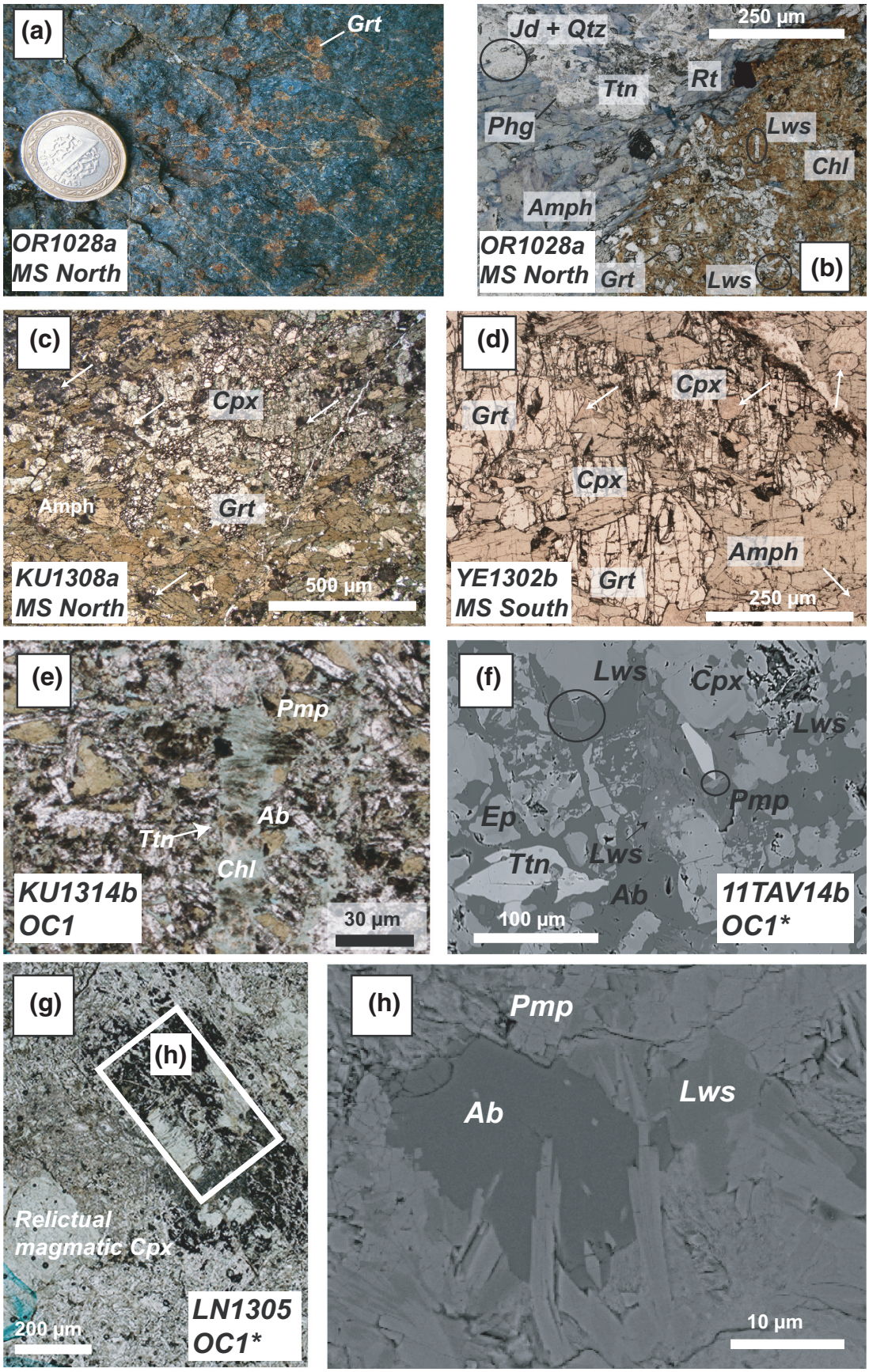


 

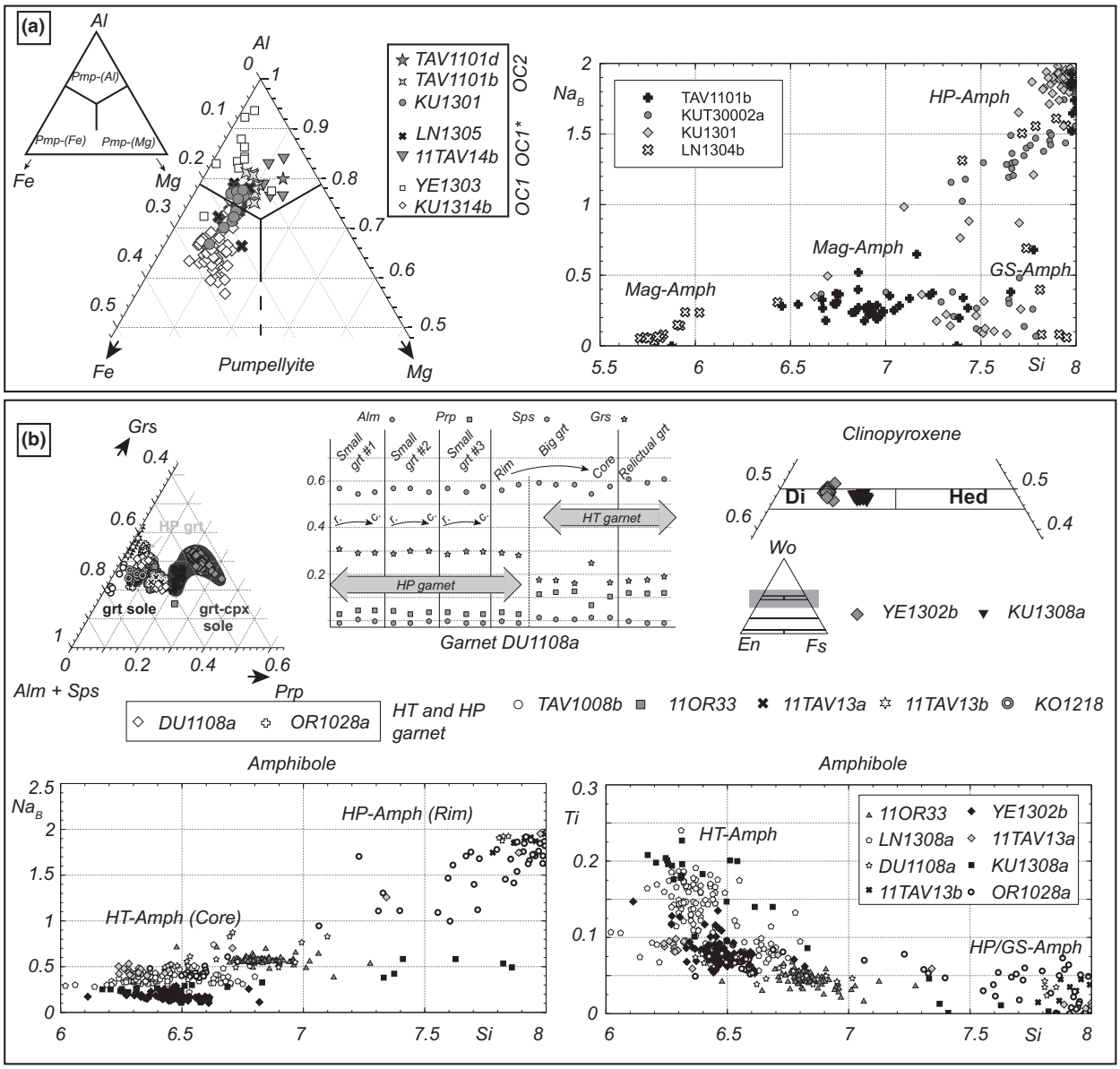


**Fig. 4** (a) Composition of pumpellyite, following the nomenclature of Passaglia and Gottardi (1973), and amphibole in samples of the oceanic units. (b) Amphibole, garnet and clinopyroxene compositions in H*T* metabasalt of the metamorphic sole. Same mineral abbreviations as in Fig. 3. Mag, magmatic; H*T*, high-temperature; GS, greenschist; H*P*, high-pressure.

plagioclase (OR1028a, DU1108a). Lawsonite was observed replacing garnet (Fig. 3b). Garnet overgrowths or newly formed crystals coexist with glaucophane.

## Oceanic complexes

### *OC1*

According to petrographic investigations, OC1 samples show only seafloor-related hydrothermal metamorphism and are devoid of any high-pressure metamorphism. The rocks are free of penetrative deformation and preserve their initial magmatic (Fig. 3e) or volcano-sedimentary texture. Common mineral assemblages are magmatic pyroxene, albitized plagioclase, chlorite and titanite. Chlorite is a common hydrothermal product replacing magmatic minerals or glass. Pumpellyite was observed after magmatic pyroxene or matrix with a composition between pumpellyite-Al and -Fe (Fig. 4a). Pumpellyite is, however, not diagnostic of *PT* conditions, as revealed by its presence in ocean-floor basalts (Ishizuka, 1999). Aegirine-augite was observed in rocks of OC1 (Okay, 1982; Plunder *et al.*, 2015). Its $Fe^{3+}$-rich composition does not allow us to consider it a high-pressure mineral: aegirine-rich pyroxene is also stable at very low pressure and temperature conditions (1 kbar, 190 °C; Massonne and Willner, 2008).

*OC1**

In addition to the previously mentioned assemblages OC1* reveals the presence of high-pressure phases (lawsonite, sodic amphibole; Fig 3f,h). The magmatic texture is still observable. Lawsonite develops in former plagioclase (Fig 3g,h) and is stable with pumpellyite, albite, aegirine-augite or chlorite. Aegirine-augite was observed overgrowing magmatic augite. Sodic amphibole was found overgrowing kaersutite (LN1304b). No systematically distinct structural patterns were observed between OC1 and OC1*. Occurrences of glaucophane below the Lycian peridotite, as reported by van der Kaaden (1966), may be taken as evidence for the existence of OC1* there.

*OC2*

Blueschist facies metamorphism and pervasive deformation characterize this unit. Pumpellyite-Fe to -Al was found coexisting with sodic amphibole and albite. The magmatic texture is locally preserved, and rims of sodic amphibole develop over calcic amphibole replacing augite. Sodic amphibole has a composition between glaucophane and ferroglaucophane and occasionally of magnesioriebeckite. Lawsonite is present as rectangular-shaped crystals coexisting with albite, glaucophane or sodic pyroxene. Fe–Mg carpholite was found in quartz-rich layers associated with phengite and/or chlorite.

## Thermodynamic modelling of metamorphic sole conditions

### Initial stage

Samples YE1302b and KU1308a were investigated to estimate the *PT* conditions of MS formation. They were chosen because they have no blueschist overprint and only moderate retrogression. *PT* pseudosections were calculated in the system $Na_2O$–CaO–FeO–MgO–$Al_2O_3$–$SiO_2$–$H_2O$±MnO using THERIAK/DOMINO (de Capitani and Petrakakis, 2010) with an updated version of Holland and Powell's (1998) database. Water was considered in excess to reproduce the modal amount of amphibole in the samples (~35–50%). $K_2O$ was neglected as no K-bearing phases were observed. $TiO_2$ was neglected because it is accommodated in rutile during H*T* stages. MnO was taken into account for sample YE1302b to reproduce the measured garnet composition and ensure the consistency of the garnet and clinopyroxene Fe–Mg exchange. It was neglected in sample KU1308a due to the very low amount present in garnet ($X_{Spessartine} < 0.03$). For both samples, the studied assemblage (garnet–clinopyroxene–plagioclase–amphibole) is stable over a large field (Fig. 5a,b). The *PT* conditions were refined for both samples, using the composition of garnet ($X_{Pyrope}$) and the amount of Ca or Na in clinopyroxene, to 10.5 ± 1 kbar and 800 ± 50 °C (Fig. 5).

### Blueschist facies overprint

The high-pressure overprint of the MS was studied in samples DU1108a and TAV1008. The blueschist paragenesis consists of lawsonite, glaucophane, sodic pyroxene and garnet for sample DU1108a. The *PT* conditions were refined to around 12 kbar and 425 °C based on the garnet–lawsonite stability field in metabasite and the reaction albite = jadeite + quartz (Evans, 1990; Liu and Bohlen, 1995; Ballèvre *et al.*, 2003; Davis and Whitney, 2008; Vitale-Brovarone *et al.*, 2011; Diener and Powell, 2012). The coexistence of sodic pyroxene with sodic amphibole and lawsonite in sample TAV108 indicates overprint conditions near 7 kbar and 325 °C (Fig. 5c).

## Discussion

Figure 6a shows the interpreted cross-section of the obducted ophiolite and underlying units at ~50 Ma. The MS share strikingly similar age, *PT* conditions and structure along the 200-km-long section. The *PT* conditions of the garnet–clinopyroxene MS along the transect were consistently found to be 11 ± 2 kbar and 800 ± 50 °C and 10.5 ± 1 kbar and 800 ± 50 °C for the MS of the Lycian and Tavşanlı areas respectively. Differences from previous estimates result from the use of different methods and parageneses for the peak assemblages (i.e. use of clinopyroxene; Table 1). Similar *PT* conditions for the H*T* part of the MS (~30 km) and synchronous cooling ages argue for the coeval formation of all MS below the ophiolite during a short-lived event (i.e. *c.* 90–95 Ma) in the same subduction zone (Fig. 6b). The remarkable preservation of the H*T* paragenesis and the subordinate or absent retrogression suggest fast exhumation of the MS (Hacker *et al.*, 1996). The accretion of OC1 in the wedge is loosely bracketed between the Turonian (age of the youngest radiolaria; Bragin and Tekin, 1996) and the Maastrichtian (reworking of sediments; Bernoulli *et al.*, 1974). Exhumation of the MS to shallow levels and their emplacement atop OC1 are therefore not well dated.

The *PT* estimates for the MS blueschist facies overprint point to an isobaric cooling (Fig. 5c) whose origin remains enigmatic. MS formation results from the short-lived accretion of successive slices decoupled from the downgoing slab and welded to the mantle wedge (Spray, 1984). The blueschist overprint of the MS, in the north of the studied region, could therefore result from the (rapid) cooling of the subduction zone (Fig. 6c1) and/or from the underplating of cold, blueschist facies OC2 slices below (Fig. 6c2). This latter contribution is supported by the presence of OC2 blueschists closely associated with MS in places (Elmaağacı section; Kızıltepe area, Dilek and Whitney, 1997). Whatever the exact mechanism, there is a striking contrast (Fig. 6a) between the MS of the Lycian southern ophiolite, which lack any blueschist overprint and were therefore exhumed shortly after H*T* sole formation, and those of the northern area, which were exhumed later once subduction had achieved a cold steady-state.

In order to reconcile the maximum thickness of the ophiolite in western Turkey (at least >10 km) with our estimated *PT* conditions (~30 km), we propose (i) partial MS exhumation with respect to the ophiolite base and/or (ii) thinning of the mantle wedge shortly after the formation of the MS. Such ductile shearing during subduction is consistent with the common occurrence of mylonites and pervasive deformation at the base of ophiolite peridotites (Boudier *et al.*, 1988; Soret *et al.*, 2016), and

 

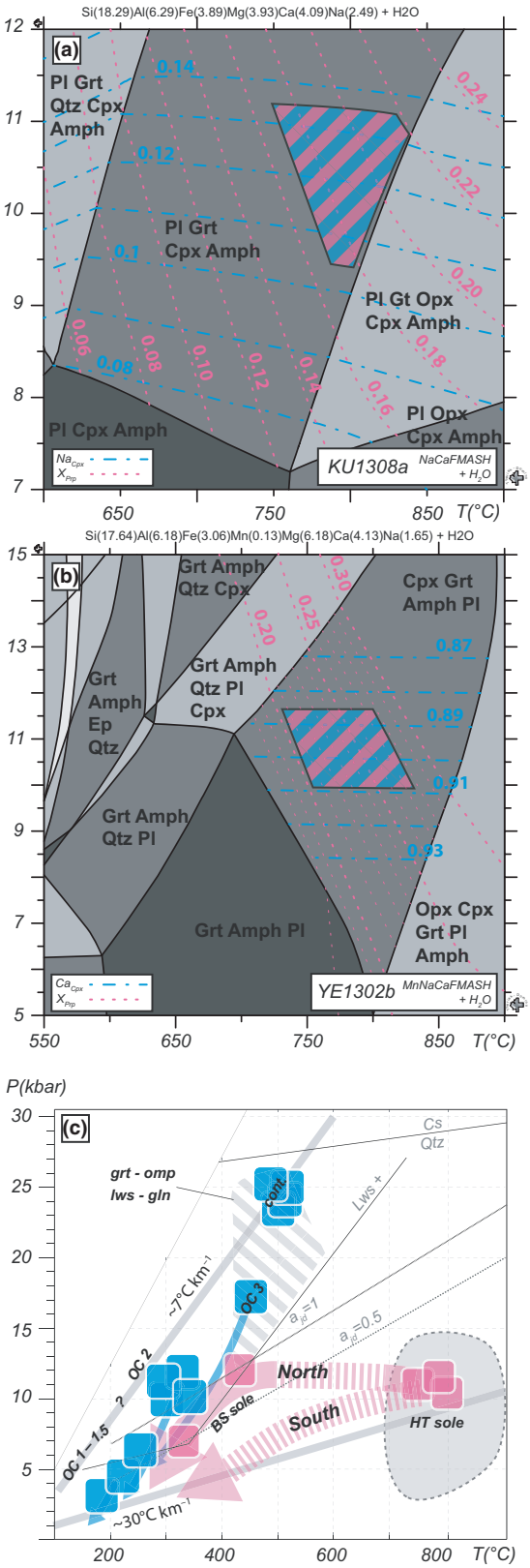


**Fig. 5** (a,b) *PT* pseudosections for samples (a) KU1308a and (b) YE1302b. Solution models used for the calculation are after Diener *et al.* (2007) for amphibole, Green *et al.* (2007) for clinopyroxene, White *et al.* (2007) for orthopyroxene, Holland *et al.* (1998) for chlorite, Baldwin *et al.* (2005) for plagioclase and Holland and Powell (1998) for garnet. (c) Summary of *PT* conditions for the oceanic and continental units investigated in the western Tavşanlı zone (Plunder *et al.*, 2015). Estimated PT conditions of the MS for the high-*T* stages (samples KU1308a and YE1302b) and the blueschist overprint (samples OR1028a and TAV1008) and the inferred *PT* path. The activity of jadeite in clinopyroxene is from Liu and Bohlen (1995), and the lawsonite stability field is after Evans (1990). Carpholite stability is after Vidal *et al.* (1992). The stability field of garnet–lawsonite–omphacite–glaucophane is after Vitale-Brovarone *et al.* (2011). Abbreviations after Kretz (1983), except for Amph, amphibole and Car, carpholite.

may reflect large-scale dynamics such as forearc extension and/or slab flattening (Dewey and Casey, 2013; van Hinsbergen *et al.*, 2015; Maffione *et al.*, 2015).

The presence of variably overprinted MS across >200 km can be explained by differences in exhumation dynamics (early vs. late) and possibly by additional exhumation-related stretching. Although most Turkish MS were rapidly exhumed after their formation (as recorded elsewhere in the world), the blueschist facies overprint on the MS indicates that parts remained at depth with oceanic units and awaited final exhumation, as most exhumed rocks from the fossil geological record (Agard *et al.*, 2009; Plunder *et al.*, 2015) or those currently underplating (Calvert, 2004).

## Acknowledgements

This work is a contribution funded through the Agence nationale de la recherche (ANR-10-BLAN-0615) granted to P.A. Detailed reviews by T. Nagel and O. Parlak were much appreciated and helped to improve the manuscript. We thank the associate editor S. Schmid for his critical remarks that strengthened the

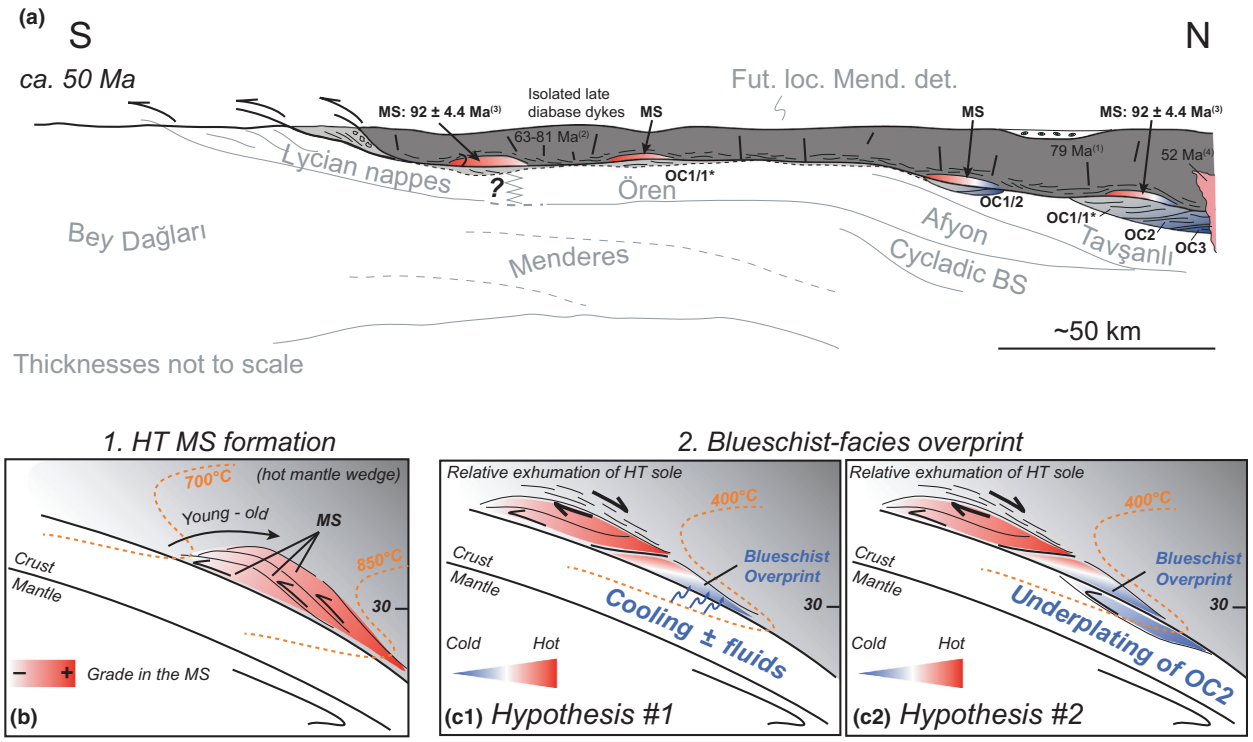


**Fig. 6** (a) Schematic representation of the ophiolite at ca. 50 Ma. Ages are from the following studies: (1) dyke of the Küthaya region (Önen, 2003); (2) dyke of the Lycian area, region of Salda (Çelik and Chiaradia, 2008); (3) cooling age of the metamorphic sole, references are given in the caption of Fig. 1; (4) age of the granodiorite emplacement in the ophiolite of the Orhaneli region (Harris *et al.*, 1994). The nummulites limestones where described north of Tavşanlı (Baş, 1986) and north of Küthaya (Özgen-Erdem *et al.*, 2007) respectively atop the peridotite and the oceanic units. (b,c1,c2) Proposed mechanism for the formation of the metamorphic sole and the blueschist overprint. Detailed explanations are given in the text.

manuscript. N. Chamot-Rooke and L. van Unnik Hoorn are greatly acknowledged for discussion of the regional geology and Fe–Mg carpholite during the preparation of this work. M. Fialin and N. Rividi from the CAMPARIS analytical platform are thanked for their help during microprobe analysis.

## References

Agard, P., Yamato, P., Jolivet, L. and Burov, E., 2009. Exhumation of oceanic blueschists and eclogites in subduction zones: timing and mechanisms. *Earth Sci. Rev.*, **92**, 53–79.

Agard, P., Yamato, P., Soret, M., Prigent, C., Guillot, S., Plunder, A., Dubacq, B., Chauvet, A. and Monié, P., 2016. Plate interface rheological switches during subduction infancy: Control on slab penetration and metamorphic sole formation. *Earth and Planetary Science Letters*. http://dx.doi.org/10.1016/j.epsl.2016.06.054

Baldwin, J.A., Powell, R., Brown, M., Moraes, R. and Fuck, R.A., 2005. Modelling of mineral equilibria in ultrahigh-temperature metamorphic rocks from the Anápolis-Itaucu Complex, central Brazil. *J. Metamorph. Geol.*, **23**, 511–531.

Ballèvre, M., Pitra, P. and Bohn, M., 2003. Lawsonite growth in the epidote blueschists from the Ile de Groix (Armorican Massif, France): a potential geobarometer. *J. Metamorph. Geol.*, **21**, 723–735.

Barrier, E. and Vrielynck, B., 2008. Atlas of Paleotectonic Maps of the Middle East (MEBE Program). CCGM-CGMW, 14 maps.

Baş, H., 1986. Tertiary geology of the Domaniç-Tavşanlı -Kütahya-Gediz region. *Jeoloji Mühendisligi*, **17**, 11–18.

Bernoulli, D., de Graciansky, P.-C. and Monod, O., 1974. The extension of the Lycian Nappes (SW Turkey) into the SE Aegean islands. *Eclogae Geol. Helv.*, **67**, 39–90.

Boudier, F., Ceuleneer, G. and Nicolas, A., 1988. Shear zones, thrusts and related magmatism in the Oman ophiolite: initiation of thrusting on an oceanic ridge. *Tectonophysics*, **151**, 275–296.

Bragin, N.Y.U. and Tekin, U.K., 1996. Age of radiolarian-chert blocks from the Senonian Ophiolitic Melange (Ankara, Turkey) . *Island Arc*, **5**, 114–122.

Brown, E.H., Wilson, D.L., Armstrong, R.L. and Harakal, J.E., 1982. Petrologic, structural, and age relations of serpentinite, amphibole, and blueschist in the Shuksan Suite of the Iron Mountain-Gee Point area, North Cascades, Washington. *Geol. Soc. Am. Bull.*, **93**, 1087–1096.

Calvert, A.J., 2004. Seismic reflection imaging of two megathrust shear zones in the northern Cascadia subduction zone. *Nature*, **428**, 163–167.

Candan, O., Çetinkaplan, M., Oberhänsli, R., Rimmelé, G. and Akal, C., 2005. Alpine high-P/low-T metamorphism of the Afyon Zone and implications for the metamorphic evolution of Western Anatolia, Turkey. *Lithos*, **84**, 102–124.

de Capitani, C. and Petrakakis, K., 2010. The computation of equilibrium assemblage diagrams with Theriak/Domino software. *Am. Mineral.*, **95**, 1006–1016.

Çelik, Ö.F., 2008. Detailed geochemistry and K-Ar geochronology of the

 

metamorphic sole rocks and their mafic dykes from the mersin ophiolite, Southern Turkey. *Turk. J. Earth Sci.*, **17**, 685–708.

Çelik, O.F. and Chiaradia, M., 2008. Geochemical and petrological aspects of dike intrusions in the Lycian ophiolites (SW Turkey): a case study for the dike emplacement along the Tauride Belt Ophiolites. *Int. J. Earth Sci.*, **97**, 1151–1164.

Çelik, Ö.F., Delaloye, M. and Feraud, G., 2006. Precise $^{40}Ar$–$^{39}Ar$ ages from the metamorphic sole rocks of the Tauride Belt Ophiolites, southern Turkey: implications for the rapid cooling history. *Geol. Mag.*, **143**, 213.

Çelik, Ö.F., Marzoli, A., Marschik, R., Chiaradia, M., Neubauer, F. and Öz, I., 2011. Early-Middle Jurassic intra-oceanic subduction in the İzmir-Ankara-Erzincan Ocean, Northern Turkey. *Tectonophysics*, **509**, 120–134.

Collins, A.S. and Robertson, A.H.F., 1997. Lycian melange, southwestern Turkey: an emplaced Late Cretaceous accretionary complex. *Geology*, **3**, 255–258.

Collins, A.S. and Robertson, A.H.F., 1998. Processes of Late Cretaceous to Late Miocene episodic thrust-sheet translation in the Lycian Taurides, SW Turkey. *J. Geol. Soc. London*, **155**, 759–772.

Daşçı, H.T., Parlak, O., Nurlu, N. and Billor, Z., 2014. Geochemical characteristics and age of metamorphic sole rocks within a Neotethyan ophiolitic mélange from Konya region (central southern Turkey). *Geodin. Acta*, **27**, 1–21.

Davis, P.B. and Whitney, D.L., 2008. Petrogenesis and structural petrology of high-pressure metabasalt pods, Sivrihisar, Turkey. *Contrib. Miner. Petrol.*, **156**, 217–241.

Dewey, J.F. and Casey, J.F., 2013. The sole of an ophiolite: the Ordovician Bay of Islands Complex, Newfoundland. *J. Geol. Soc. London*, **170**, 715–722.

Diener, J.F.A. and Powell, R., 2012. Revised activity-composition models for clinopyroxene and amphibole. *J. Metamorph. Geol.*, **30**, 131–142.

Diener, J.F.A., Powell, R., White, R.W. and Holland, T.J.B., 2007. A new thermodynamic model for clino- and orthoamphiboles in the system Na2O-CaO-FeO-MgO-Al2O3-SiO2-H2O-O. *J. Metamorph. Geol.*, **25**, 631–656.

Dilek, Y. and Whitney, D.L., 1997. Counterclockwise P-T-t trajectory from the metamorphic sole of a Neo-Tethyan ophiolite (Turkey). *Tectonophysics*, **280**, 295–310.

Dilek, Y., Thy, P., Hacker, B. and Grundvig, S., 1999. Structure and petrology of Tauride ophiolites and mafic dike intrusions (Turkey): implications for the Neotethyan ocean. *Geol. Soc. Am. Bull.*, **111**, 1192–1216.

Dora, O.Ö., Candan, O., Kaya, O., Koralay, E. and Dürr, S., 2001. Revision of 'Leptite-gneisses' in the Menderes Massif: a supracrustal metasedimentary origin. *Int. J. Earth Sci.*, **89**, 836–851.

Evans, B.W., 1990. Phase relations of epidote-blueschists. *Lithos*, **25**, 3–23.

Gessner, K., Collins, A.S., Ring, U. and Güngör, T., 2004. Structural and thermal history of poly-orogenic basement: U-Pb geochronology of granitoid rocks in the southern Menderes Massif, Western Turkey. *J. Geol. Soc. London*, **161**, 93–101.

de Graciansky, P.-C., 1972. *Recherches Géologiques dans le Taurus Lycien Occidental*. Universite de Paris-Sud, Orsay, France.

Green, E., Holland, T. and Powell, R., 2007. An order-disorder model for omphacitic pyroxenes in the system jadeite-diopside-hedenbergite-acmite, with applications to eclogitic rocks. *Am. Mineral.*, **92**, 1181–1189.

Hacker, B.R., 1994. Rapid emplacement of young oceanic lithosphere: argon geochronology of the Oman ophiolite. *Science*, **265**, 1563–1565.

Hacker, B.R. and Gnos, E., 1997. The corundrum of Samail: explaining metamorphic history. *Tectonophysics*, **279**, 215–226.

Hacker, B.R., Mosenfelder, J.L.L. and Gnos, E., 1996. Rapid emplacement of the Oman ophiolite: thermal and geochronogic constraints. *Tectonics*, **15**, 1230–1247.

Harris, N.B.W., Kelley, S. and Okay, A.I., 1994. Post-collision magmatism and tectonics in northwest Anatolia. *Contrib. Miner. Petrol.*, **117**, 241–252.

van Hinsbergen, D.J.J., Kaymakci, N., Spakman, W. and Torsvik, T.H., 2010. Reconciling the geological history of western Turkey with plate circuits and mantle tomography. *Earth Planet. Sci. Lett.*, **297**, 674–686.

van Hinsbergen, D.J.J., Peters, K., Maffione, M., Spakman, W., Guilmette, C., Thieulot, C., Plümper, O., Gürer, D., Brouwer, F.M., Aldanmaz, E., Kaymakcı, N., Basset, D. and Watts, A., 2015. Dynamics of intraoceanic subduction initiation: 2. Suprasubduction zone ophiolite formation and metamorphic sole exhumation in context of absolute plate motions. *Geochem. Geophys. Geosyst.*, **16**, 1771–1785.

van Hinsbergen, D.J.J., Maffione, M., Plunder, A., Kaymakcı, N., Ganerød, M., Hendriks, B.W.H., Corfu, F., Gürer, D., de Gelder, G.I.N.O., Peters, K., McPhee, P.J., Brouwer, F.M., Advokaat, E.L. and Vissers, R.L.M., 2016. Tectonic evolution and paleogeography of the K ı r ş ehir Block and the Central Anatolian Ophiolites, Turkey. *Tectonics*, **35**, 983–1014.

Holland, T.J.B. and Powell, R., 1998. An internally consistent thermodynamic data set for phases of petrological interest. *J. Metamorphic Geol.*, **16**, 309–343.

Holland, T.J.B., Baker, J. and Powell, R., 1998. Mixing properties and activity-composition relationships of chlorites in the system MgO-FeO-AlO-SiO2-H2O. *Eur. J. Mineral.*, **10**, 395–406.

Ishizuka, H., 1999. Pumpellyite from the oceanic crust, DSDP/ODP Hole 504B. *Mineral. Mag.*, **63**, 891–900.

van der Kaaden, G., 1966. The signifiance and distribution of glaucophane rocks in Turkey. *Bull. Mineral. Res. Explor. Inst.*, **67**, 37–67.

Kretz, R., 1983. Symbols for rock-forming minerals. *Am. Mineral.*, **68**, 277–279.

Lisenbee, A., 1972. *Structural Setting of the Orhaneli Ultramafic Massif Near Bursa, Northwestern Turkey*. Pennsylvania State University, USA, 158 pp.

Liu, J. and Bohlen, S.R., 1995. Mixing properties and stability of jadeite-acmite pyroxene in the presence of albite and quartz. *Contrib. Miner. Petrol.*, **119**, 433–440.

Maffione, M., van Hinsbergen, D.J.J., Koornneef, L.M.T., Guilmette, C., Hodges, K., Borneman, N., Huang, W., Ding, L. and Kapp, P., 2015. Forearc hyperextension dismembered the south Tibetan ophiolites. *Geology*, **43**, 475–478.

Manav, H., Gültekin, A.H. and Uz, B., 2004. Geochemical evidence for the tectonic setting of the Harmancik ophiolites, NW Turkey. *J. Asian Earth Sci.*, **24**, 1–9.

Massonne, H.-J. and Willner, A.P., 2008. Phase relations and dehydration behaviour of psammopelite and mid-ocean ridge basalt at very-low-grade to low-grade metamorphic conditions. *Eur. J. Mineral.*, **20**, 867–879.

Okay, A.I., 1982. Incipient Blueschist Metamorphism and Metasomatism in the Tavşanlı Region, Northwest Turkey. *Contrib. Miner. Petrol.*, **79**, 361–367.

Okay, A.I. and Tüysüz, O., 1999. Tethyan sutures of northern Turkey. *Geol. Soc. London Spec. Publ.*, **156**, 475–515.

Okay, A.I., Harris, N.B.W. and Kelley, S., 1998. Exhumation of blueschists

 

along a Tethyan suture in northwest Turkey. *Tectonophysics*, **285**, 275–299.
Önen, P., 2003. Neotethyan ophiolitic rocks of the Anatolides of NW Turkey and comparison with Tauride ophiolites. *Geol. Soc. London Spec. Publ.*, **160**, 947–962.
Önen, A.P. and Hall, R., 1993. Ophiolites and related metamorphic rocks from the Kutahya region, north-west Turkey. *Geol. J.*, **28**, 399–412.
Önen, P. and Hall, R., 2000. Sub-ophiolite metamorphic rocks from NW Anatolia, Turkey. *J. Metamorph. Geol.*, **18**, 483–495.
Özgen-Erdem, N., Akyazı, M. and Karabaşoğlu, A., 2007. Biostratigraphic interpretation and systematics of Alveolina assemblages from the Ilerdian-Cuisian limestones of Southern Eskişehir, Central Turkey. *J. Asian Earth Sci.*, **29**, 911–927.
Parlak, O. and Delaloye, M., 1996. Geochemistry and timing of post-metamorphic dyke emplacement in the Mersin Ophiolite (southern Turkey): new age constraints from 40Ar/39Ar geochronology. *Terra Nova*, **8**, 585–592.
Passaglia, E. and Gottardi, C., 1973. Crystal chemistry and nomenclature of pumpellyites and julgoldites. *Can. Mineral.*, **IX**, 219–223.
Plunder, A., Agard, P., Chopin, C., Pourteau, A. and Okay, A.I., 2015. Accretion, underplating and exhumation along a subduction interface: from subduction initiation to continental subduction (Tavşanlı zone, W. Turkey). *Lithos*, **226**, 233–254.
Poisson, A., 1977. *Recherches Géologiques dans les Taurides Occidentales (Turquie)*. Université Paris-Sur, Orsay, 795 pp.
Pourteau, A., Candan, O. and Oberhänsli, R., 2010. High-pressure metasediments in central Turkey: constraints on the Neotethyan closure history. *Tectonics*, **29**, TC5004.
Pourteau, A., Bousquet, R., Vidal, O., Plunder, A., Duesterhoeft, E., Candan, O. and Oberhänsli, R., 2014. Multistage growth of Fe–Mg–carpholite and Fe–Mg–chloritoid, from field evidence to thermodynamic modelling. *Contrib. Miner. Petrol.*, **168**, 1090.
Pourteau, A., Oberhänsli, R. Candan, O., Barrier, E. and Vrielynck, B., 2016. Neotethyan closure history of western Anatolia: a geodynamic discussion. *International Journal of Earth Science*, **105**, 203. doi: 10.1007/s00531-015-1226-7
Şengör, A.M.C. and Yılmaz, Y., 1981. Tethyan evolution of Turkey: a plate tectonic approach. *Tectonophysics*, **75**, 181–241.
Soret, M., Agard, P., Dubacq, B., Vitale-Brovarone, A., Monié, P., Chauvet, A., Whitechurch, H. and Villemant, B., 2016. Strain localization and fluid infiltration in the mantle wedge during subduction initiation: evidence from the base of the New Caledonia ophiolite. *Lithos*, **244**, 1–19.
Spray, J.G., 1984. Possible causes and consequences of upper mantle decoupling and ophiolite displacement. *Geol. Soc. London Spec. Publ.*, **13**, 255–268.
Thuizat, R., Whitechurch, H., Montigny, R. and Juteau, T., 1981. K-Ar dating of some infra-ophiolitic metamorphic soles from the Eastern Mediterranean: new evidence for oceanic thrustings before obduction. *Earth Planet. Sci. Lett.*, **52**, 302–310.
Topuz, G., Okay, A.I., Altherr, R., Meyer, H.-P. and Nasdala, L., 2006. Partial high-pressure aragonitization of micritic limestones in an accretionary complex, Tavşanlı Zone, NW Turkey. *J. Metamorph. Geol.*, **24**, 603–613.
Vidal, O., Goffé, B. and Theye, T., 1992. Experimental study of the stability of sudoite and magnesiocarpholite and calculation of a new petrogenetic grid for the system FeO-MgO-$Al_2O_3$-$SiO_2$-$H_2O$. *J. Metamorph. Geol.*, **10**, 603–614.
Vitale-Brovarone, A., Groppo, C., Hetényi, G., Compagnoni, R. and Malavieille, J., 2011. Coexistence of lawsonite-bearing eclogite and blueschist: phase equilibria modelling of Alpine Corsica metabasalts and petrological evolution of subducting slabs. *J. Metamorph. Geol.*, **29**, 583–600.
Wakabayashi, J. and Dilek, Y., 2003. What constitute 'emplacement' of an ophiolite?: mechanisms and relationship to subduction initiation and formation of metamorphic soles. *Geol. Soc. London Spec. Publ.*, **218**, 427–447.
White, R.W., Powell, R. and Holland, T.J.B., 2007. Progress relating to calculation of partial melting equilibria for metapelites. *J. Metamorph. Geol.*, **25**, 511–527.
Whitechurch, H., Juteau, T. and Montigny, R., 1984. Role of the Eastern Mediterranean ophiolites (Turkey, Syria, Cyprus) in the history of the Neo-Tethys. *Geol. Soc. London Spec. Publ.*, **17**, 301–317.

*Received 16 February 2016; revised version accepted 22 June 2016*

## Supporting Information

Additional Supporting Information may be found in the online version of this article:

**Figure S1.** Detail section of the location reported on Fig. 2 (a) Devlez-Tavşanlı section; (b) Orhaneli section; (c) Elmaağacı section; (d) Murat dağ section; (e) Iğdir-Belkaya section; (f) Yayla-Datça section. Inset: general section with location of the detail sections.

**Table S1.** GPS coordinate of samples from this study and assemblage.

**Table S2.** representative microprobe analysis and formula unit from selected samples.

**Appendix S1.** Outcrop and section description. Analytical procedure.

 